

# SENSORLESS SPEED AND DIRECT TORQUE CONTROL OF INTERIOR PERMANENT MAGNET SYNCHRONOUS MACHINES BASED ON EXTENDED KALMAN FILTER

Mihai CERNAT, Vasile COMNAC, Florin MOLDOVEANU

Faculty of Electrical Engineering, *Transilvania* University of Brasov, Romania

**Abstract** – The application of vector control techniques in a.c. drives demands accurate position and speed feedback information for the current control and servo-control loops. The paper describes a digital sensorless speed control system for Interior Permanent Magnet Synchronous Machines (IPMSM). A Kalman filter is used to estimate the mechanical state of the motor.

## I. INTRODUCTION

Basically, there are two main techniques for the instantaneous torque control of high-performance variable speed drives: vector control and Direct Torque Control (DTC). The main advantages of DTC are: the absence of coordinate transformations, the absence of a separate voltage modulation block and of a voltage decoupling circuit and a reduced number of controllers. However, on the other hand, this solution requires knowledge of the stator flux, electromagnetic torque, angular speed and position of the rotor. Recently, a strong interest was shown in the alternative PMSM sensorless control using stator voltage and current measurements only, based on state observers. Luenberger and Gopinath type state observers traditionally yield very good results in the estimation of linear systems state parameters. However, the application of these estimation procedures to a.c. machines systems and drives show a weaker performance, the main cause being the strongly non-linear model of a.c. machines. The Extended Kalman Filter (EKF) is a state observer specially designed for non-linear systems. Existing literature

features numerous applications of Kalman filters to achieve sensorless control of asynchronous machines [5], or d.c.-brushless machines [6], or permanent magnet synchronous machines [1-4, 7].

This paper presents the development of an EKF specially designed for the sensorless direct torque control of an IPMSM. The main difficulty in developing a Kalman filter for an IPMSM is caused by the complexity of the dynamic model, which is more complicated than that of the Surface PMSM, due to the asymmetry of the magnetic circuit. This excludes from the very beginning for an IPMSM the use of a dynamic model with parameters in the fixed reference frame  $\alpha - \beta$  attached to the stator, as used for the implementation of a Kalman filter for a SPMSM [2].

The simplified block diagram of the proposed extended Kalman filter-based control system is shown in Fig. 1.

The superscript \* (star) denotes reference quantities.

The IPMSM drive control is carried out using a conventional VSI-fed DTC system that employs two hysteresis controllers for directly selecting (in each sampling period) the optimal voltage switch vector (there are six non-zero and two zero vectors). The I+PI speed controller gives the reference value of the electromagnetic torque ( $m_e^*$ ). The Kalman filter generates the estimated values of the stator linkage flux, the actual rotor angular velocity and the stator flux space vector position, using the measured values of the currents and voltages at the motor terminals.

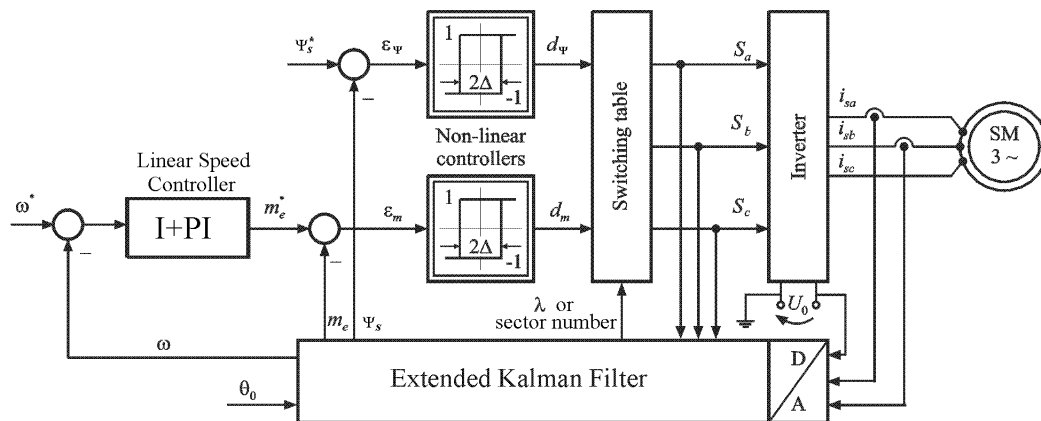


Fig. 1. Extended Kalman Filter Based Control System for IPMSM

## I. THE KALMAN FILTER

The Kalman filter is in principle a state observer that establishes the best approximation for the state variables of a system, by minimization of the square error, subjected at both its input and output to random disturbances. If the dynamic system of which the state is being observed is non-linear, then the Kalman filter is called an extended one (EKF). The development of the Kalman filter is closely linked to the stochastic systems. The linear stochastic systems are described by relations:

$$\dot{\mathbf{x}}(t) = \mathbf{A} \mathbf{x}(t) + \mathbf{B} \mathbf{u}(t) + \mathbf{w}(t), \quad \mathbf{x}(t_0) = \mathbf{x}_0, \quad (1)$$

$$\mathbf{y}(t) = \mathbf{C} \mathbf{x}(t), \quad (2)$$

$$\mathbf{z}(t) = \mathbf{y}(t) + \mathbf{v}(t), \quad (3)$$

where:

$\mathbf{x}$ ,  $\mathbf{y}$ ,  $\mathbf{u}$ ,  $\mathbf{A}$ ,  $\mathbf{B}$ ,  $\mathbf{C}$  have the significance known from deterministic systems [1, 2];

$\mathbf{w}(t)$  represents the vector of disturbances applied at the system input;

$\mathbf{z}(t)$  is the vector of the measurable outputs, affected by the random noise  $\mathbf{v}(t)$ .

It can be considered that, besides the input disturbances, vector  $\mathbf{w}(t)$  includes some uncertainties referring to the process model. It will be assumed that the vector functions  $\mathbf{w}(t)$  and  $\mathbf{v}(t)$  are not correlated and zero-mean stochastic processes. From statistic point of view, the stochastic processes  $\mathbf{w}(t)$  and  $\mathbf{v}(t)$  are characterized by the covariance matrices  $\mathbf{Q}$  and  $\mathbf{R}$  respectively. It is further assumed that the initial state  $\mathbf{x}_0$  is a vector of random variables, of mean  $\bar{\mathbf{x}}_0$  and covariance  $\mathbf{P}_0$ , not correlated with the stochastic processes  $\mathbf{w}(t)$  and  $\mathbf{v}(t)$  over the entire interval of estimation.

The covariance matrices  $\mathbf{Q}$ ,  $\mathbf{R}$ ,  $\mathbf{P}_0$ , characterizing the noise sources of system (1)–(3) are, by definition, symmetrical and positively semi-definite, of dimensions  $(n \times n)$ ,  $(m \times m)$  and  $(n \times n)$  respectively, where  $n$  and  $m$  represent the number of state and output variables, respectively.

For linear time invariant systems, the following relations of recurrent computation describe the general form of the Kalman filters implementation algorithm:

$$\mathbf{K}_k = \mathbf{P}_k |_{k-1} \mathbf{C}^T (\mathbf{C} \mathbf{P}_k |_{k-1} \mathbf{C}^T + \mathbf{R})^{-1}, \quad (4)$$

$$\hat{\mathbf{x}}_k |_{k-1} = \hat{\mathbf{x}}_k |_{k-1} + \mathbf{K}_k (\mathbf{y}_k - \mathbf{C} \hat{\mathbf{x}}_k |_{k-1}), \quad (5)$$

$$\mathbf{P}_k |_{k-1} = (\mathbf{I}_n - \mathbf{K}_k \mathbf{C}) \mathbf{P}_k |_{k-1}, \quad (6)$$

$$\hat{\mathbf{x}}_{k+1} |_{k-1} = \mathbf{A}_d \hat{\mathbf{x}}_k |_{k-1} + T_s \mathbf{B} \mathbf{u}_k, \quad (7)$$

$$\mathbf{P}_{k+1} |_{k-1} = \mathbf{A}_d \mathbf{P}_k |_{k-1} \mathbf{A}_d^T + \mathbf{Q}, \quad (8)$$

where the quantity  $T_s$  represents the sampling period, and  $\mathbf{A}_d$  is the matrix of the discrete linearised system, expressed by:

$$\mathbf{A}_d = \mathbf{I}_n + T_s \mathbf{A}. \quad (9)$$

In these relationships, the  $(n \times m)$  matrix  $\mathbf{K}$  represents the Kalman gain,  $\mathbf{P}$  represents the covariance state matrix and  $\mathbf{I}_n$  is the  $(n \times n)$  unit matrix. In the recurrent computation relationships, the subscript index notations of type  $k | k-1$  show that the respective quantities (state vectors or their covariance matrices) are computed for sample  $k$ , using the values of similar quantities from the previous sample.

For non-linear stochastic systems, the dynamic state model is described by the following expressions:

$$\dot{\mathbf{x}}(t) = \mathbf{f}(\mathbf{x}(t), \mathbf{u}(t), t) + \mathbf{w}(t), \quad (10)$$

$$\mathbf{y}(t) = \mathbf{h}(\mathbf{x}(t), t), \quad (11)$$

$$\mathbf{z}(t) = \mathbf{h}(\mathbf{x}(t), t) + \mathbf{v}(t), \quad (12)$$

where  $\mathbf{f}$  and  $\mathbf{h}$  are  $(n \times 1)$  and  $(m \times 1)$  function vectors, respectively. The  $\mathbf{A}$  and  $\mathbf{C}$  matrices of the EKF structure are dependent now upon the state of the system and are determined by:

$$\mathbf{A}(\hat{\mathbf{x}}(t), t) = \left. \frac{\partial \mathbf{f}(\mathbf{x}(t), \mathbf{u}(t), t)}{\partial \mathbf{x}^T(t)} \right|_{\mathbf{x}(t) = \hat{\mathbf{x}}(t)} \quad (13)$$

$$\mathbf{C}(\hat{\mathbf{x}}(t), t) = \left. \frac{\partial \mathbf{h}(\mathbf{x}(t), t)}{\partial \mathbf{x}^T(t)} \right|_{\mathbf{x}(t) = \hat{\mathbf{x}}(t)} \quad (14)$$

Additionally to the fact that matrices  $\mathbf{A}$  and  $\mathbf{C}$  have now became dependent on the state of the system, the algorithm suffers some further changes, which affect relationships (5) and (7), now expressed as:

$$\hat{\mathbf{x}}_k |_{k-1} = \hat{\mathbf{x}}_k |_{k-1} + \mathbf{K}_k [\mathbf{y}_k - \mathbf{h}(\hat{\mathbf{x}}_k |_{k-1})], \quad (15)$$

$$\hat{\mathbf{x}}_{k+1} |_{k-1} = \mathbf{x}_k |_{k-1} + T_s \mathbf{f}(\hat{\mathbf{x}}_k |_{k-1}, \mathbf{u}_k). \quad (16)$$

The Kalman filter algorithm is initiated by adopting adequate values for the covariance matrix of the initial state  $\mathbf{P}_0 = \mathbf{P}_{0|-1}$ , as well as for the weighting matrices  $\mathbf{Q}$  and  $\mathbf{R}$ , the latter two being constant during the estimation.

## III. MACHINE MODEL FOR DEVELOPMENT OF THE EXTENDED KALMAN FILTER

The studied IPMSM is assumed to have a symmetrical three-phase, star-connected, isolated neutral point stator winding. The model is developed according to some simplifying assumptions, therefore saturation and iron losses (hysteresis) are not considered. The induced electromotive force is assumed to have a sinusoidal waveform, while eddy currents are neglected. Since excitation is provided by permanent magnets, there is no variation of field currents and there is no rotor cage. Permanent magnets are buried in the rotor steel, so the machine is characterized by a cylindrical asymmetry causing the phase direct stator inductance  $L_d$  to be lower than the quadrature one  $L_q$ . The on-line implementation computations of the EKF algorithm will be considerably simplified if the dynamic model of the IPMSM is expressed in the rotating rotor reference frame, with axis  $d$  oriented along the north pole direction of the magnet. The state variables of the model deterministic part are included in vector:

$$\mathbf{x} = [\Psi_d \ \Psi_q \ \omega \ \theta]^T, \quad (17)$$

where  $\Psi_d$  and  $\Psi_q$  are the direct and the quadrature components of the stator flux space vector in relation to the rotor frame, and  $\omega$  and  $\theta$  represent the rotor (mechanical) angular velocity and position, respectively. The input quantities of the process (the IPMSM in this case) are the components of the vector

$$\mathbf{u} = [u_d \ u_q \ m_l]^T, \quad (18)$$

where quantities  $u_d$  and  $u_q$  are the direct and quadrature components of the stator voltage space phasors, and quantity  $m_l$  represents the load torque. In order to ensure an interface of the EKF with the directly measurable quantities at the machine terminals, in the estimation model components  $u_d$  and  $u_q$  are expressed as functions of the stator voltage phasor components in the fixed two-phase frame  $\alpha$ - $\beta$  using relations:

$$u_d = u_\alpha \cos p\theta + u_\beta \sin p\theta; \quad (19a, b)$$

$$u_q = -u_\alpha \sin p\theta + u_\beta \cos p\theta$$

where  $p$  is the number of pole pairs and voltages  $u_\alpha$  and  $u_\beta$  are given by relations:

$$u_\alpha = u_a, \quad u_\beta = (u_a + 2u_b) / \sqrt{3}, \quad (20a, b)$$

where  $u_a$  and  $u_b$  are the instantaneous values of the phase stator voltages.

Under these circumstances, the deterministic part of the dynamic model of the IPMSM written in the standard form specified by relation (10) will be [1, 2]:

$$\mathbf{f}(\mathbf{x}(t), \mathbf{u}(t)) = [f_1 \ f_2 \ f_3 \ f_4]^T, \quad (21)$$

where:

$$f_1 = -\frac{R_s}{L_d} \Psi_d + p\omega \Psi_q + \frac{R_s}{L_d} \Psi_e + u_\alpha \cos p\theta + u_\beta \sin p\theta$$

$$f_2 = -p\omega \Psi_d - \frac{R_s}{L_q} \Psi_q - u_\alpha \sin p\theta + u_\beta \cos p\theta$$

$$f_3 = (k_{m1} \Psi_d \Psi_q + k_{m2} \Psi_q - D\omega - m_l) / J$$

$$f_4 = \omega \quad (21 a, b, c, d)$$

$$k_{m1} = \frac{3}{2} p \left( \frac{1}{L_q} - \frac{1}{L_d} \right); \quad k_{m2} = \frac{3}{2} \frac{p \Psi_e}{L_d}, \quad (22)$$

where  $R_s$  is the stator resistance,  $\Psi_e$  is the permanent magnet linkage flux,  $J$  is the inertia and  $D$  is the viscous damping factor.

The selection of the output quantities is the most important stage in the development of the EKF proposed by this paper. These quantities will have a double expression. Thus, in order to ensure an as simple as possible interface of the EKF with the process, the output quantities comprised by vector:

$$\mathbf{y} = [i_\alpha \ i_\beta]^T, \quad (23)$$

will be adopted, where  $i_\alpha$  and  $i_\beta$  are the current space vector components in the fixed two-phase reference frame.

They can be obtained as function of the measurable quantities  $i_a$  and  $i_b$  with relationships similar to expressions (19). On the other hand, the output quantities (23) will be expressed as functions of the state variables (11), thus obtaining the non-linear output function of the deterministic part of the state variable model:

$$\mathbf{y} = \mathbf{h}(\mathbf{x}(t)) = \begin{bmatrix} \frac{\Psi_d - \Psi_e}{L_d} \cos p\theta - \frac{\Psi_q}{L_q} \sin p\theta \\ \frac{\Psi_d - \Psi_e}{L_d} \sin p\theta + \frac{\Psi_q}{L_q} \cos p\theta \end{bmatrix}. \quad (24)$$

Based on the previous elements, the EKF can now be built and applied to the IPMSM. By derivation of the vectorial function (21) in relation to the state vector, and then by applying relation (14), matrix  $\mathbf{A}_d$  of the discrete linearised system will be obtained:

$$\mathbf{A}_d = \begin{bmatrix} A_d^{11} & A_d^{12} \\ A_d^{21} & A_d^{22} \end{bmatrix}, \quad (25)$$

with

$$A_d^{11} = \begin{bmatrix} 1 - T_s \frac{R_s}{L_d} & p\omega T_s \\ -p\omega T_s & 1 - T_s \frac{R_s}{L_q} \end{bmatrix},$$

$$A_d^{12} = \begin{bmatrix} p \Psi_q T_s & p T_s (-u_\alpha \sin p\theta + u_\beta \cos p\theta) \\ -p \Psi_d T_s & -p T_s (u_\alpha \cos p\theta + u_\beta \sin p\theta) \end{bmatrix}$$

$$A_d^{21} = \begin{bmatrix} T_s \frac{k_{m1} \Psi_q}{J} & T_s \frac{k_{m1} \Psi_d + k_{m2}}{J} \\ 0 & 0 \end{bmatrix},$$

$$A_d^{22} = \begin{bmatrix} 1 - T_s \frac{D}{J} & 0 \\ T_s & 1 \end{bmatrix}. \quad (25 a, b, c, d)$$

Matrix  $\mathbf{C}$  of the EKF algorithm will follow, considering relation (19), by derivation of vector function  $\mathbf{h}$  of expression (24) in relation to the state variables:

$$\mathbf{C} = \begin{bmatrix} \frac{\cos p\theta}{L_d} & -\frac{\sin p\theta}{L_q} & 0 & -p \left( \frac{\Psi_d - \Psi_e}{L_d} \sin p\theta + \frac{\Psi_q}{L_q} \cos p\theta \right) \\ \frac{\sin p\theta}{L_d} & +\frac{\cos p\theta}{L_q} & 0 & +p \left( \frac{\Psi_d - \Psi_e}{L_d} \cos p\theta - \frac{\Psi_q}{L_q} \sin p\theta \right) \end{bmatrix} \quad (26)$$

#### IV. THE CONTROL STRUCTURE

The simplified block diagram of the EKF-based control system is shown in Fig. 1. The control system, consist of two parallel loops for direct torque and stator flux control and an outer loop for the linear control of the rotor angular velocity.

##### THE DIRECT TORQUE AND FLUX CONTROL

This part of the control system contains two non-linear,

hysteresis controllers and a functional block labeled “Switching table”, that generate binary signals  $S_a$ ,  $S_b$  and  $S_c$  applied to the inverter branches. For  $S_i = 1$ , the transistors of the branch  $i = a, b, c$ ,  $T_i^+$  and  $T_i^-$  (Fig. 2), are switched on and off, respectively and for  $S_i = 0$  the two transistors are inverse switched.

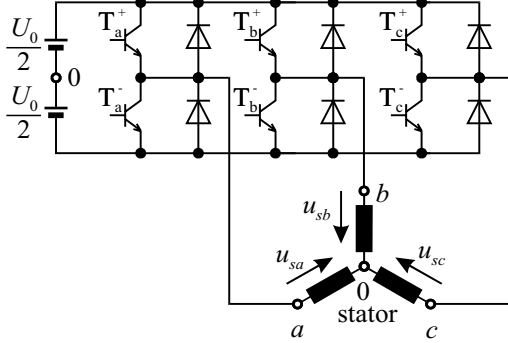


Fig. 2. The power part of the studied drive system.

The switching state of the inverter ( $S_a S_b S_c$ ) is achieved in two steps. Firstly, based on outputs  $d_\psi$  and  $d_m$  of the non-linear controllers and angle  $\lambda$  of the stator flux vector, according to Table 1 [2, 3] a stator voltage space vector is selected. Then, with this space vector, based on Table 2, is achieved the switching state of the inverter.

Table 1: Switching logic of the three-phase inverter, for different positions of the stator flux vector

$\lambda$	$d_q$	1	-1	-1	1
	$d_m$	1	1	-1	-1
$-30^\circ \div 30^\circ$		$\underline{U}_2$	$\underline{U}_3$	$\underline{U}_5$	$\underline{U}_6$
$30^\circ \div 90^\circ$		$\underline{U}_3$	$\underline{U}_4$	$\underline{U}_6$	$\underline{U}_1$
$90^\circ \div 150^\circ$		$\underline{U}_4$	$\underline{U}_5$	$\underline{U}_1$	$\underline{U}_2$
$150^\circ \div 210^\circ$		$\underline{U}_5$	$\underline{U}_6$	$\underline{U}_2$	$\underline{U}_3$
$210^\circ \div 270^\circ$		$\underline{U}_6$	$\underline{U}_1$	$\underline{U}_3$	$\underline{U}_4$
$270^\circ \div 330^\circ$		$\underline{U}_1$	$\underline{U}_2$	$\underline{U}_4$	$\underline{U}_5$

Table 2: Relations between switching states and voltage space vectors (VSV).

VSV	$S_a$	$S_b$	$S_c$
$\underline{U}_1$	1	0	0
$\underline{U}_2$	1	1	0
$\underline{U}_3$	0	1	0
$\underline{U}_4$	0	1	1
$\underline{U}_5$	0	0	1
$\underline{U}_6$	1	0	1
$\underline{U}_7$	0	0	0
$\underline{U}_8$	1	1	1

## THE ANGULAR VELOCITY CONTROLLER

The angular velocity controller has an important influence on the entire control system performance, both during transient and steady state regimes. Good performance could be achieved using an I type control law for the angular velocity reference quantity  $\omega^*$ , and a PI control law for the angular velocity feedback  $\omega$  respectively. The I+PI controller will operate with both these laws. The main advantage of an I+PI controller is the achievement of good transient performance. At the same time, due to the unitary discrete pole, a null stationary error with respect to the perturbation of the load torque (including the friction torque of the machine) is achieved. It can be noticed that the integration uses the trapeze method.

The controller algorithm, obtained by applying the inverse Z transform, is described by recurrent equations:

$$\varepsilon_\omega(n) = \omega^*(n) - \omega(n), \quad (27)$$

$$x_\omega(n) = x_\omega(n-1) + \frac{T_{e\omega}}{2 T_{r\omega}} [\varepsilon_\omega(n) - \varepsilon_\omega(n-1)], \quad (28)$$

$$m_e^*(n) = k_{r\omega} [x_\omega(n) - \omega(n)], \quad (29)$$

where:  $\varepsilon_\omega, x_\omega$  - the auxiliary variables associated to the angular velocity loop error and to the integrator respectively;  $k_{r\omega}, T_{r\omega}$  - the tuning parameters of the angular velocity controller,  $n$  - the index of the sampling period  $T_{e\omega}$ . The tuning parameters of the speed controller are computed with the following relations [2]:

$$k_{r\omega} = J / (4 T_\mu k_\omega), \quad T_{r\omega} = 8 T_\mu, \quad (30)$$

where  $T_\mu$  is the time constant of the first order delay element that models the control loop of the electromagnetic torque.

## V. ANALYSIS OF THE KALMAN FILTER-BASED CONTROL SYSTEM

In order to analyze the dynamic behavior of the control system with a Kalman filter, simulations were conducted in C++. Normal operation circumstances were taken into consideration, the estimated quantities being connected as reaction quantities to the digital current and angular velocity controllers. The feedback quantities,  $m_e$  and  $\Psi_s$ , are obtained through numerical computation, based on relationships:

$$m_e = k_{m1} \hat{\Psi}_d \hat{\Psi}_q + k_{m2} \hat{\Psi}_q, \quad \Psi_s = \sqrt{\hat{\Psi}_d^2 + \hat{\Psi}_q^2}, \quad (31a, b)$$

where  $k_{m1}, k_{m2}$  are constants determined with (22 a, b). The model of the simulated machine considers the load torque and the viscous friction torque respectively:  $m_{lN} = 1$  Nm,

$D_N = 0.002$  Nms/rad. The rated data of the motor employed for simulation are:  $p = 2$ ,  $R_{sN} = 0.98 \Omega$ ,  $L_{dN} = 9.1$  mH,

$L_{qN} = 18$  mH,  $\Psi_{eN} = 0.174$  Wb;  $J_N = 0.006$  Kg m<sup>2</sup>. The sampling periods are of 2 ms for the angular velocity controller and of 0.1 ms for the stator flux and electromagnetic torque control loops and also for the Kalman filter.

It is assumed that the reference quantity for the angular velocity has a trapezoidal waveform, specific for servo-drives with incremental motion. As previously shown, in order to optimise the dynamic behaviour of the Kalman filter, it is required to adopt adequate values for the elements of the square matrices  $P_0$ ,  $Q$  and  $R$ . In the paper the following values were adopted:  $P_0 = 0.01 I_4$ ,  $Q = 0.00002 I_4$  and  $R = 0.9 I_2$ . In order to highlight the performances of the Kalman filter control system, the behaviour of the direct torque digital control system in absence of a Kalman filter is presented initially.

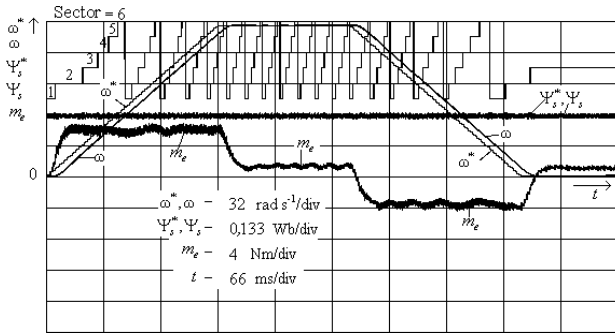
Fig. 4 shows the waveforms of the stator flux amplitude (reference, real and estimated) and mechanical (fig. 4a) and electrical (fig. 4b) quantities respectively, obtained for a DTC system without EKF for a precise tuning of the velocity controller. The same quantities, obtained for the control system with an EKF are presented in fig. 5. A comparison of figures 4 and 5 shows insignificant modifications in the

dynamic behaviour of the controller, this validating the EKF-based control system.

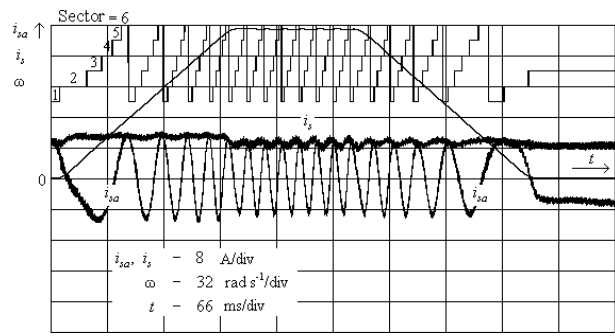
The wave forms from Fig. 6a have been obtained for a mismatch of the model electrical parameters values ( $R_s = 1.7 R_{sN}$ ,  $L_d = 0.7 L_{dN}$ ,  $L_q = 0.7 L_{qN}$  and  $\Psi_e = 0.8 \Psi_{eN}$ ) related to the rated values used for tuning of the speed controller and for EKF. Fig. 6b illustrate the dynamic behavior of the Kalman filter-based control system obtained for an incorrect initialization of the estimated position.

Figures 7 a, b was obtained for a simultaneous mismatch of the inertia, damping factor and load torque related to the rated values:  $J = 0.7 J_N$ ,  $D = 0.5 D_N$ ,  $m_l = 0.5 m_{lN}$  (Fig. 7a) and  $J = 1.4 J_N$ ,  $D = 2 D_N$ ,  $m_l = 1.5 m_{lN}$  (Fig. 7b).

In these figures,  $\Delta\omega = \omega - \hat{\omega}$ ,  $\Delta\theta = \theta - \hat{\theta}$  are the estimation errors of the angular velocity and position, respectively.

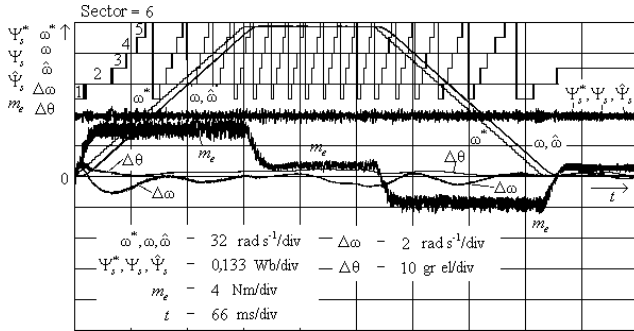


a)

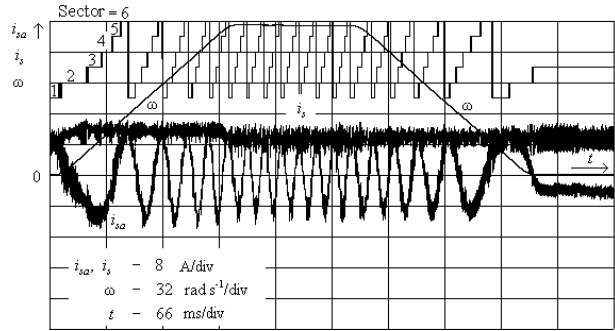


b)

Fig. 4.

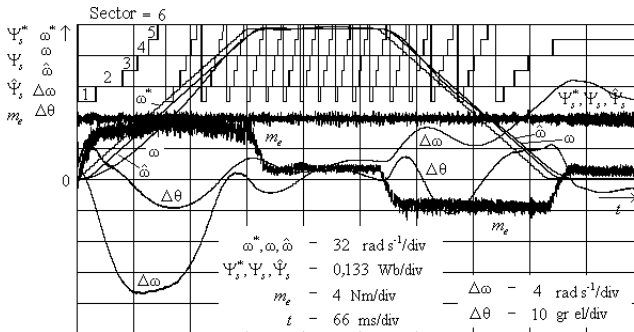


a)

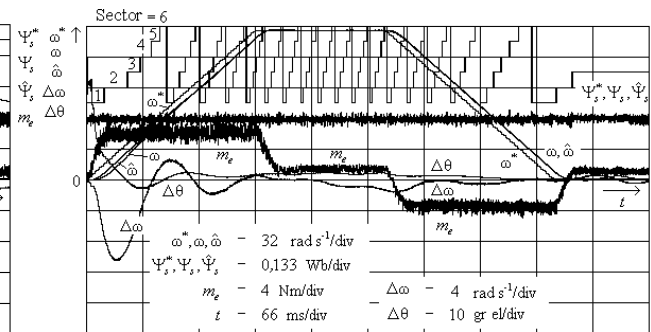


b)

Fig. 5.



a)



b)

Fig. 6.

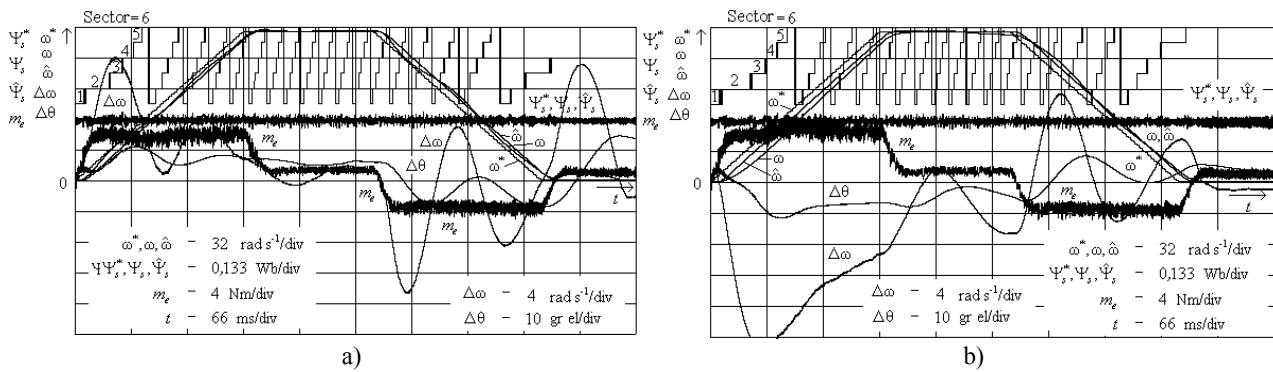


Fig. 7.

## VI. CONCLUSION

The paper presents the development of a mechanical sensorless digital control system of the rotor angular velocity of an IPMSM. The estimation of the mechanical state quantities of the drive system is made using an extended Kalman filter. The paper studies the interaction between the observer and the closed loop control system. The simulation shows that the dynamic behaviour of the Kalman filter based control system is good even if the electric and mechanic parameters of the machine are different from the rated values used for the design of the controllers and the Kalman filter and also if there is an incorrect initialization of the estimated position.

## 7. References

- [1] Vas, P.: *Sensorless Vector and Direct Torque Control*. Oxford University Press (UK), 1998.
- [2] Comnac V.: *Contributions to the Study of Incremental Motion Drive Systems with Permanent Magnet Synchronous Machines*, Doctoral thesis, Transilvania University of Brasov, 1998.
- [3] Dhaouadi R., Mohan N.: *Application of Stochastic Filtering to a Permanent Magnet Synchronous Motor Drive System without Electro-Mechanical Sensors*. Proceedings of International Conference on Electrical Machines ICEM, Cambridge-Massachusetts (USA), 1990, pp.1225-1230
- [4] Liu S., Stiebler, M.: *State Estimation of PWM Inverter's Fed Synchronous Motor by Using Stochastic Filtering Techniques*. Proceedings of International Conference on Electrical Machines ICEM, Cambridge-Massachusetts (USA), 1990, pp.1206-1211
- [5] Beierke S., Vas P., Simor B., Stronach A.F.: *DSP-Controlled Sensorless AC Vector Drives Using Extended Kalman Filter*. Proceedings of the International Conference on Power Electronics and Motion Control PCIM 97, Nuremberg (Germany), June 1997, pp. 31-41
- [6] Kettle P., Murray A., Moynihan F.: *Sensorless Control of a Brushless DC Motor Using an Extended Kalman Estimator*. International Conference on Power Electronics and Motion Control PCIM 98, Nuremberg (Germany), May 1998, pp. 385-392
- [7] Comnac V., Moldoveanu F., Cernat M., Draghici I., Cernat R.-M.: *Sensorless Control of Interior Permanent Magnet Synchronous Machine Using Stochastic Filtering Techniques*. Proceedings of the 7th International Conference on Optimization of Electrical and Electronic Equipment - OPTIM 2000, Brasov (Romania), 11 - 12 May 2000, Vol. 3, pp. 619-624.